

Citation for published version:
Price, GJ & Ansari, DM 2003, 'An inverse gas chromatography study of calcination and surface modification of kaolinite clays', *Physical Chemistry Chemical Physics*, vol. 5, no. 24, pp. 5552-5557. https://doi.org/10.1039/b309641f

DOI:

10.1039/b309641f

Publication date: 2003

Document Version Peer reviewed version

Link to publication

# **University of Bath**

#### **Alternative formats**

If you require this document in an alternative format, please contact: openaccess@bath.ac.uk

Copyright and moral rights for the publications made accessible in the public portal are retained by the authors and/or other copyright owners and it is a condition of accessing publications that users recognise and abide by the legal requirements associated with these rights.

Take down policy
If you believe that this document breaches copyright please contact us providing details, and we will remove access to the work immediately and investigate your claim.

Download date: 09. Mar. 2023

# AN INVERSE GAS CHROMATOGRAPHY STUDY OF CALCINATION AND SURFACE MODIFICATION OF KAOLINITE CLAYS

Gareth J. Price a,\* and Deeba M. Ansari a,b

- <sup>a</sup> Dept. of Chemistry, University of Bath, Claverton Down, BATH, BA2 7AY, U.K. and
- b Imerys Minerals Ltd., John Keay House, St Austell, Cornwall, PL25 4DJ, UK
- \* To whom correspondence and proofs should be addressed. E-mail: g.j.price@bath.ac.uk

#### **ABSTRACT**

Inverse gas chromatography, IGC, has been used to investigate the surface properties of a kaolinite clay. Changes in enthalpies of adsorption for a range of probes and in the surface energies of the clays have been measured and the effect of calcination of the native clay as well as of coating with an amino- propylsilane coupling agent have been determined. The surface energy of the clay was lowered by calcination and further considerably reduced on coating with the silane. From the retention of polar probes, information on the accessibility of surface sites to the probes and on the acid-base character of the surface was measured. Two commonly used methods for quantifying these specific interactions are compared and yield similar results. The hydrated clay became less porous and less acidic after calcination while coating with the silane conferred a largely, though not exclusively, basic character.

**Keywords:** Inverse Gas Chromatography; kaolin, calcined clay; surface energy; surface modification.

#### **INTRODUCTION**

Kaolin, or china clay, is found in many parts of the world and is an important commercial product. Among its uses is as a mineral filler in a range of polymer composite materials. In these applications, an understanding of the interactions between the polymer and the clay is important for predicting composite performance and thus characterisation of the clay surfaces is needed, particularly in terms of its surface energy. These values can be obtained by, for example, liquid adsorption measurements, 1,2 flow microcalorimetry 3 or contact angle measurements 4 but these methods are not easily and widely applicable and the latter difficult to use with finely divided solids. A number of workers have demonstrated the usefulness of Inverse Gas Chromatography, IGC, for investigating the surface energies of a range of mineral solids 5.

In IGC the solid under investigation is packed into a column over which an inert carrier gas flows. Small amounts of "probe" solvents are injected into the carrier and the retention time depends on the interactions between the probe and the surface. By using probes with a range of properties, the nature of the surface can be defined with good accuracy. The technique was formerly mainly applied to polymers<sup>5,6</sup> and this work continues<sup>7</sup> but more recently IGC been used to characterise the properties of a range of surfaces including silicas and activated carbons<sup>8</sup>, filler materials and pigments<sup>9–11</sup> and pharmaceutical agents.<sup>12, 13</sup>

Clays are aluminosilicates with a structures<sup>14</sup> consisting of layers of octahedral and tetrahedral arrangements of oxygen atoms around aluminium and silicon respectively.

Different clays have different lattice structures; kaolinite has the octahedra and tetrahedra in a 1:1 ratio arranged in layers<sup>15</sup> and has the general formula Al<sub>2</sub>O<sub>3</sub>.2SiO<sub>2</sub>.2H<sub>2</sub>O. Cation exchange can take place to modify the chemistry of the clay. This is particularly prevalent for natural clays where some variation in composition and hence properties is expected.

These hydrated structures undergo rearrangement on heating to form two further widely used minerals<sup>16</sup>. Above 500 °C, dehydroxylation occurs endothermically to form metakaolin. By 650 °C, approximately 90 % of the dehydroxylation is complete<sup>15</sup>. Metakaolin has a highly reactive surface, probably due to an increase in the number of Lewis sites, with reduction in the coordination of aluminium. On further heating, to above 980 °C, a defect spinel structure arises forming 'calcined clay'. Calcined clay is much less reactive than metakaolin, but isolated hydroxyl groups are retained on the surface and may undergo coupling reactions<sup>15</sup>.

In order to assist dispersion and adhesion when used as a filler in a polymer matrix, it is often necessary to treat the surface of the clay with a dispersion or coupling agent<sup>17</sup>. In addition, extraction and processing of clays involves the use of refining and improving chemicals, such as floatation and bleaching agents. The effect of each of these treatments on the surface properties has to be taken into account in terms of the performance of the filler.

Some clay minerals have previously been studied using IGC in an attempt to determine the effects of chemical modification. Bandosz *et al.* studied<sup>18</sup> the effect of introducing large metal polycations to form pillared smectites (a 2:1 clay) which were useful as catalysts, adsorbents or molecular sieves. Alkane and alkene probes were used show that, after calcination, the Lewis acid sites were reduced with lower  $\pi$ -bonding interactions. The study was extended<sup>19</sup> to include surface polymerisation and carbonisation as well as<sup>20</sup> the effect of heat treatment or high temperature reaction with propylene on taeniolites. In other work, montmorillonite and bentonite<sup>21</sup> matrices were also modified by a similar technique and the sorption properties of the surfaces characterised.

Illites (another 2:1 clay) and kaolinites are important in the petrochemical industry since they comprise the majority of subsoils in oilfields and their wettability is related to the retention of heavy oils. The surface properties of some illites from various origins were

measured by Saada et al. using IGC where the use of branched alkane probes allowed characterisation of the surface morphology<sup>22</sup>. This was later<sup>23</sup> extended to use a finite concentration technique to characterise the heterogeneity of the clay surfaces.

Both hydrous and calcined clays are used in preparing composites with polyolefins and polyamides and we are engaged in a programme investigating the properties of these polymer composites. Despite the work outlined above, there has been no systematic study of measuring the thermodynamic changes on calcination and dehydroxylation and/or the surface treatment of a kaolinite and the effects on mechanical properties of composites when used as a filler. In this paper, we present an investigation of a kaolinite and its modification. Two commonly used methods of treating IGC data to determine surface energies are compared using the results from the interaction of a range of probes with kaolinites.

#### **EXPERIMENTAL**

*Materials:* The kaolin sample (termed here as **HYC** – <u>HY</u>drated <u>C</u>lay) was a high-purity china clay extracted from a commercial site in Cornwall, UK and was washed and refined without the use of processing chemicals. The calcined clay (termed **CAC** – <u>CA</u>lcined <u>C</u>lay) was a commercially available grade (Polestar 200R, Imerys Minerals) which was modified from the original feedclay by calcining at 1100 °C. Characterisation details of both materials are given in Table 1.

A third material, termed here **CAC-Sil**, was produced by silylation of the calcined clay. Because of its commercial application for dispersing calcined clays in polyamide composites, the silane modifier used was  $\gamma$ -aminopropyl triethoxysilane, NH<sub>2</sub>–(CH<sub>2</sub>)<sub>3</sub> –Si-(O-C<sub>2</sub>H<sub>5</sub>)<sub>3</sub> (A1100 from Witco). The calcined clay was coated with a calculated monolayer amount of silane in a Steele and Cowlishaw high-speed mixer for fifteen minutes. The ethanol

formed as a bi-product was removed by conditioning in an air circulating oven for three days at 60 °C.

To prepare packings for IGC, the clays were pressed into pellets using a press at 20 t pressure, then crumbled and sieved to give aggregates of  $425 - 850 \,\mu\text{m}$ . These were packed with the aid of mechanical agitation into washed stainless steel columns of  $\frac{1}{4}$  in o.d. Columns of length  $0.90 - 1.0 \,\text{m}$  which contained  $10 - 12 \,\text{g}$  of packing were used. The columns were pre-conditioned in a slow flow of carrier gas at  $150 \,^{\circ}\text{C}$  for 24 hours, before further conditioning for twelve hours at the measurement temperature.

Chromatography: A Perkin-Elmer Autosystem XL gas chromatograph employing FID detection was used. The column temperature was measured to  $\pm$  0.2 °C on a Chrompack RDT thermometer that was calibrated against an NPL calibrated Tinsley Type 5840 platinum resistance thermometer. Looped-valve tubing before the column inlet permitted the inlet pressure and flow to be measured to  $\pm$  0.3 cm<sup>3</sup> min<sup>-1</sup> with a FP-407 (Chrompack) solid state calibrated dual flow and pressure meter. Oxygen-free nitrogen was used as the carrier gas and was passed through a Perkin-Elmer three-stage drying and purification system, before entering the chromatograph. The barometric pressure was measured at the beginning and end of each run using a BDH precision aneroid barometer; the mean of the two was used for all calculations. The instrument was located in a temperature-controlled laboratory, maintained at 23 °C  $\pm$  1 °C.

After conditioning, a series of  $\sim 0.1 \mu L$  aliquots of the vapour of the probes used were injected by Hamilton syringe over a range of temperatures. All probes were chromatographic grade (BDH). Retention times were recorded and processed by the PE-Nelson Turbochrom data management software. Methane was used as a non-interacting marker to determine the void volume of the column. Each value reported is the result of at least three elutions agreeing to within experimental uncertainty. In order to confirm that the results were collected at

infinite dilution, injections of n-pentane were made with varying sample sizes in the range  $0.01-0.1\mu L$  and over a range of flow rates. Repeated injections of volumes between 0.01 and  $0.05~\mu L$  gave retention times with no significant variation within the experimental uncertainty. There was no dependence on carrier flow rates between 20 and 50 cm<sup>-3</sup> min<sup>-1</sup>.

### RESULTS AND DISCUSSION

The primary measurement in IGC is the net retention volume,  $V_{\text{n}}$ , given  $^{22}$  by

$$V_n = J f(t_r - t_0)$$
 (1)

where  $t_r$  is the retention time taken for the probe,  $t_0$  that for the non-interacting marker and f is the carrier gas flow rate corrected to S.T.P. J is the correction factor for pressure drop across the column and carrier gas compressibility, given with the column inlet and outlet pressures,  $p_i$  and  $p_o$  respectively by:

$$J = \frac{3}{2} \left[ \frac{(p_i / p_0)^2 - 1}{(p_i / p_0)^3 - 1} \right]$$

For solid minerals, absorption into the bulk is negligible and retention is solely due to adsorption onto the solid surface. It can readily be shown<sup>24</sup> that  $V_n$  is related to the Gibbs energy of adsorption for the probe onto the surface,  $\Delta G_a^{\circ}$ , by:

$$\Delta G_a^{\circ} = -RT \ln \left( \frac{V_n p_g}{\pi W_s S_a} \right)$$
 or  $\Delta G_a^{\circ} = -RT \left[ \ln(V_n) + (constant) \right]$  (2)

where  $S_a$  is the specific surface area of the adsorbent,  $W_s$  the weight of sample in the column,  $\pi$  is the surface pressure of the liquid probe and  $p_g$  the equilibrium vapour pressure of the probe under standard conditions. Using the approach of De Boer<sup>25</sup> which has commonly been adopted in defining the standard states,  $\Delta G_a{}^{\circ}$  can be calculated over a series of temperatures from measurement of  $V_n$  and since

$$\Delta G^{\circ}_{a} = \Delta H^{\circ}_{a} - T \Delta S^{\circ}_{a} = -RT \ln V_{n} + k$$
(3)

if  $\Delta G^{\circ}_{a}$  is plotted *versus* T, the isosteric (zero coverage) enthalpy of adsorption can be calculated from the intercept and the corresponding entropy change from the slope, with the assumption that both parameters do not depend on temperature over the range investigated.

This approach was applied to the three clay samples and  $\Delta G^{\circ}_{a}$  calculated for each probe over a range of temperatures. The values are plotted for each of the clays investigated in Figures 1 – 3. The derived enthalpies and entropies of adsorption are given in Tables 2 and 3 respectively.

The values of  $\Delta H^{\circ}_{a}$  for the native hydrated clay are comparable with previously published data for native kaolinites and illites. Saada et al.<sup>22</sup> studied three kaolinites from different sources, ΔH<sub>a</sub> for hexane varying from 49 to 62 kJ mol<sup>-1</sup> compared with 59 kJ mol<sup>-1</sup> found here. The Literature values shown in Table 2 were for a heritage formation ground kaolinite and are in excellent agreement with the measurements reported here. The  $\Delta H^{\circ}$ <sub>3</sub> for alkanes after calcination fell by between 9 to 13 kJ mol<sup>-1</sup>. This reduction may be explained by considering the changes that occur during calcination. On heating to > 1000 °C, structural changes result in a more ordered layer structure and loss of hydroxyl groups from the surface. This gives a reduction in polarity and hence in the adsorption enthalpies. The values for the silane coated clay showed a larger variation with the size of the alkane. Pentane and hexane gave  $\Delta H^{\circ}_{a}$  values comparable with CAC although they were significantly lower for heptane and octane. This may signify some steric constraints on adsorption of the longer alkanes. This last suggestion is also supported by the  $\Delta S_a^{\circ}$  values. There is little variation for the adsorption of pentane but a greater loss of entropy is involved in the adsorption of the longer alkanes on the hydrated clays than the dehydrated versions presumably due to the stronger interactions restricting the number of adoptable sites and conformations on the surface.

Following the approach pioneered by Fowkes<sup>26</sup> the surface energy of the solid,  $\gamma_s$  can be split into two components, one due to van der Waals or dispersion forces,  $\gamma_s^d$ , and one due to other specific interactions such as polar, acid-base etc.,  $\gamma_s^{sp}$ 

$$\gamma_s^d = \gamma_s^d + \gamma_s^{sp} \tag{4}$$

The non-specific or dispersive component of the substrate surface energy,  $\gamma_s^d$ , can be calculated from the elution data for saturated hydrocarbon probes, which are assumed to interact only by dispersion intermolecular forces. The free energy change for the adsorption of a single methylene group,  $\Delta G^{\circ}_a$ ,  $^{CH_2}$ , is found from the difference in free energies of adsorption for succeeding alkanes in an homologous series

$$\Delta G_{a}^{\circ, CH_{2}} = RT \ln \left( \frac{V_{n}^{\circ}(n+1)}{V_{n}^{\circ}(n)} \right)$$
 (5)

where n is the number of carbons in the linear alkane.  $\gamma_s^{\ d}$  can then be calculated from  $^{27,\,28}$ 

$$\gamma_{\rm s}^{\rm d} = \frac{1(-\Delta G_a^{\circ,CH_2})^2}{\gamma_{CH_2}(2Na_{CH_2})}$$
 (6)

where N is Avogadro's number;  $\gamma_{CH2}$  is the surface tension of a hypothetical surface containing only methylene groups and  $a_{CH2}$  is the cross-sectional area of a methylene group ( $\approx 0.06 \text{ nm}^2$ ). Thus at constant temperature, for a series of alkane probes, a plot RT ln ( $V_n$ ) versus the number of carbon atoms should give a straight line from which  $\Delta G^{\circ}_{a}{}^{,CH_2}$  can be found. It is clear that this will not give an exact value of  $\gamma_s{}^d$  under all circumstances since, for example,  $a_{CH2}$  will be somewhat temperature dependent. However, comparison of relative results across a series of systems should allow reasonable conclusions as to the surface behaviour to be made and this has become an accepted method for comparing surface adsorptions  $^{10, 29, 30}$ . The plot for HYC is shown in Figure 4. Those for CAC and CAC-Sil are very similar in appearance and are given in Figures S1 and S2 of supplementary material to

this paper. All show the expected linear relationship and the values of  $\gamma_s^{\ d}$  calculated are given in Table 4.

The results were comparable to the lowest data of Saada *et al.*<sup>22</sup>, recorded for a finely ground clay. These authors suggested that at least some of the variation in retention resulted from differences in surface area and porosity. The kaolinites studied by Saada *et al.* had surface areas ranging from 14 to 40 m<sup>2</sup>g<sup>-1</sup> compared with 8.8 m<sup>2</sup>g<sup>-1</sup> for the HYC used here; clays with high surface areas are more porous and may retain small probes more strongly leading to higher surface free energy results. They postulated that lower results for agraded (processed) clays were due to a more uniform surface. The lower results in this work for CAC compared with HYC, support this suggestion.

The value of  $\gamma_s^d$  represents the interaction of the surface with an alkane and hence is a measure of how easily the surface can polarise the probe. At the infinite dilution conditions involved in this IGC work, the probes will interact most strongly with the high surface energy sites so, for a heterogeneous surface, the  $\gamma_s^d$  results will predominantly reflect these, rather than being an average across the whole surface.

As detailed above, after calcination the surface structure of kaolinite is altered with high-energy hydroxyl sites being removed. This is reflected in the reduction in the measured surface free energy. Clay surfaces are strongly acidic, related to layer defects and hydroxyl and oxygen atoms in the aluminate structures and silicate layers<sup>31</sup>. Strong Lewis acids are formed by cations of interlayer materials and this has led to a range of applications, for example in chemical synthesis<sup>32</sup>. On calcination, these sites are altered as the interlayered structure collapses and a proportion of the highest energy surface sites are removed. However, there is still some hydroxyl functionality present so that a relatively high energy surface remains.

A markedly greater lowering of  $\gamma_s^d$  occurs on treatment with the aminosilane. Alkoxysilanes react primarily with hydroxyl functionality. The reduction in  $\gamma_s^d$  clearly bears this out. For this silane, reaction of the basic amine with the acidic surface might be expected. However, the chain length is short and so reaction only at one end of the molecule is possible, that of the silane terminus being favoured. An completely alkane-like surface would have a  $\gamma_s^d$  of 30-35 mJ sm<sup>-2</sup> so that it is clear that some functionality remains on the surface, albeit at a greatly reduced energy compared with CAC.

To calculate the  $\gamma_s^{sp}$  contribution from Equation (4), a selection of other non-alkane probes was used at 100 °C. Two methods have been used in the Literature to determine the specific interaction parameters.

In the first method<sup>28</sup>, it is assumed that the dispersive components are given by

$$\Delta G_a = 2 \left( \gamma_s^d \gamma_L^d \right)^{1/2} \tag{7}$$

where  $\gamma_s^d$  and  $\gamma_L^d$  are the surface energies for the solid and probe liquid respectively. From Equations (3) and (5), this is equivalent to

- RT 
$$lnV_n = 2N (\gamma_s^d)^{\frac{1}{2}} a(\gamma_L^d)^{\frac{1}{2}} + constant$$
 (8)

so that by plotting RT  $lnV_n$  against  $a(\gamma_L^d)^{\frac{1}{2}}$  the slope corresponds to the response of a non-polar (alkane) probe. If a polar probe is used, with an equivalent value of  $a(\gamma_L^d)^{\frac{1}{2}}$ , the deviation from the alkane line on the RT $lnV_n$  axis will be equivalent to  $\Delta G^o_{\text{specific}}$ . This method requires knowledge of the probe surface tension and its contact area, a. These are not always readily obtained but in this work the data for the probes were taken from data by Shultz and Lavielle<sup>33</sup>.

A second, empirical method for estimating specific interactions was also applied, as suggested by Saint-Flour and Papirer<sup>34, 35</sup>. In this,  $\Delta G^o_a$  is plotted against the saturated vapour pressure of the probe liquid,  $p^o$ , which is readily obtained from literature. The results for the alkane probes are again used to determine a reference line. Given the nature of the alkanes,  $p^o$ 

is a reflection of the strength of dispersion forces. Deviations from the line will be due to specific interaction energies and the difference between probes allows estimation of the interaction type and strength. While there are difficulties in assigning exact quantitative significance to the values obtained, useful comparative information can be obtained. In particular, use of probes with acidic (acceptor), basic (donor) and amphoteric properties allows conclusions to be drawn on the nature of the solid.

The plots arising from these two treatments for HYC hydrated clay are shown in Figures 5 and 6. The resulting interaction energies are shown in Table 5. Agreement between the two methods used was generally good except for the amphoteric probes acetone and ethyl acetate. Values arising from the 'log P°' plot were somewhat lower although the trends in both data sets were the same. Reasons for the non-agreement probably arise from uncertainties in the values of a and  $\gamma_L^d$  at the temperature of measurement. While the vapour pressure method does not give absolute measures of the interaction energies, the data is more readily available for a range of probes and should allow comparison of a set of results for different surfaces. The method was therefore used for the two other clays studied and the results are also shown in Table 4.

Generally, interactions with polar probes on CAC were lower than for HYC or could not be detected within our experimental protocols either giving extremely long retention times or very broad and heavily skewed peaks, making determination of the precise retention time impossible. Those polar probes not detected were either retained over an excessive period, or underwent some chemisorption at the surface, and could not be removed. THF and diethyl ether are highly basic probes while acetone and ethyl acetate have both acid and base character. Given the highly acidic nature of the clays, it is perhaps not surprising that these compounds interacted very strongly with the surfaces.

There are negative apparent interaction energies for cyclohexane and carbon tetrachloride, implying lower interaction than with the corresponding alkane. In the former case, the nature of the interactions interactions would be the same and the lower value is presumably due to steric factors preventing the bulkier cyclohexane from accessing sites that are available to the linear compound. The same argument can be made for the relatively bulky CCl<sub>4</sub> probe. Thus the results for these probes may reflect changes in the morphology of the surface in addition to changes in its chemical nature. The degree of porosity and/or intercalation would be lower in the treated clays. Depending on its orientation at the surface, chloroform could also present a surface area similar to that of CCl<sub>4</sub>.

Specific interaction energies for the alkenes hexene and octene for CAC were approximately half of those compared with HYC and those for CAC-Sil even lower. These probes are Lewis bases through  $\pi$ -interaction and the trend of results indicates a lowering of the acidic nature of the surface with treatment.

On silane treatment specific interactions change from acidic, electron acceptor-type to those of basic, electron donor-type. Thus specific interaction results for the acids, carbon tetrachloride and chloroform were negative for CAC and positive for CAC-Sil. Results for the alkenes showed the opposite effect, with a reduction in specific interaction energy on surface modification. These data are consistent with the presence of some functional amine group at the mineral surface. It is also known that some siloxane functionality is introduced due to hydrolysis of the triethoxysilane. In other work<sup>36</sup> we have shown that surface modification with long chain alkyl carboxylic acids effectively produces and alkane-like layer at the surface with  $\gamma_s^d$  values in the region of 30 mJ m<sup>-2</sup>. These surface modifications have a large influence on the performance of the clays as fillers in a thermoplastic composite and results in this area will be described in a separate publication.<sup>37</sup>.

# **CONCLUSIONS**

Our results further validate the use of IGC for the study of the surface properties of finely divided solids. Changes to the surface structure and properties of a native kaolinite clay have been measured as a result of calcination and of coating with an aminopropylsilane coupling agent. The enthalpies of adsorption of alkane probes and the dispersive component of surface free energy were reduced by calcination and further considerably reduced on coating with the silane. By investigating the retention of polar probes, information on the accessibility of surface sites to the probes and on the acid-base character of the surface was measured. The hydrated clay became less porous and less acidic on calcinations while coating with the silane conferred a largely, though not exclusively, basic character.

#### REFERENCES

- 1. I. Dekany *Pure Appl. Chem.* **64,** 1499, (1992)
- 2. I. Dekany and L.G. Nagy Colloids and Surfaces 58, 252, (1990)
- 3. D. P. Ashton and R. N. Rothan *Controlled Interfaces in Composite Materials*. Elsevier, Amsterdam (1990)
- 4. P. M. Costanzo, R. F. Giese and C. J. van Oss (1991). in K. L. Mittal and H. R. Anderson (Eds), *Acid-base interactions: relevance to adhesion science and technology*, VSP.
- 5. D. R. Lloyd, T. C. Ward and H. P. Schreiber (Eds) (1989). *Inverse Gas Chromatography: Characterisation of Polymers and Other Materials*, Amer. Chem. Soc., Washington DC
- 6. Z. Y. Al-Saigh and J. E. Guillet (2000). Inverse Gas Chrmoatography in the Analysis of Polymers and Rubbers in R. Meyers (Ed), in *Encyclopedia of Analytical Chemistry: Instrumentation and Applications*, Wiley, pp. 7759
- 7. R. P. Danner, F. Tihminlioglu, R. K. Surana and J. L. Duda *Fluid Phase Equilib.* **148**, 171, (1998).
- 8. E. Papirer, E. Brendle, F. Ozil and H. Balard *Carbon* **37**, 1265, (1999).
- 9. A. Lundqvist and L. Odberg *J. Pulp Pap. Sci.* **23,** J298, (1997).
- 10. H. Balard and E. Papirer *Prog. Org. Coat.* **22,** 1, (1993).
- 11. D. S. Keller and P. Luner Colloid Surf. A-Physicochem. Eng. Asp. 161, 401, (2000).
- 12. B. C. Hancock and S. L. Shamblin *Pharm. Sci. Technol. Today* 1, 345, (1998).
- 13. M. D. Ticehurst, R.C. Rowe and P. York *Int. J. Pharm.* **111,** 241, (1994).
- 14. G. Sposito *The chemistry of soils*. Oxford University Press, New York (1989)
- 15. R. E. Grim *Clay Mineralogy*. McGraw-Hill, New York (1968)
- 16. G. W. Brindley and D. M. Moroney J. Amer. Ceram. Soc. 43, 511, (1960).
- 17. L. E. Nielsen and R. F. Landel *Mechanical Properties of Polymers and Composites* 2nd Edn. Marcel Dekker, New York (1994)

- 18. T. J. Bandosz, J. Jagiello, K. A. G. Amankwah and J. A. Schwarz *Clay Min.* **27,** 435, (1992).
- 19. T. J. Bandosz, J. Jagiello, B. Andersen and J. A. Schwarz Clay Min. 40, 306, (1992).
- 20. T. J. Bandosz, J. Jagiello and J. A. Schwarz J. Chem. Soc.-Faraday Trans. 92, 4631, (1996).
- 21. B. Hamdi, Z. Kessaissia, J. B. Donnet and T. K. Wang *Ann. Chim.-Sci. Mat.* **24,** 63, (1999).
- 22. A. Saada, E. Papirer, H. Balard and B. Siffert J. Colloid Interface Sci. 175, 212, (1995).
- 23. H. Balard, A. Saada, E. Papirer and B. Siffert Langmuir 13, 1256, (1997).
- 24. J. R. Conder and C. L. Young *Physicochemical measurement by gas chromatography*. Wiley, New York (1978)
- 25. J. H. de Boer *The dynamic character of adsorption*. Clarendon Press, Oxford (1953)
- 26. F. M. Fowkes Ind. Eng. Chem. Prod. Res. Dev. 56, 40, (1967).
- 27. J. H. Park, Y. K. Lee and J. B. Donnet *Chromatographia* **33**, 154, (1992).
- 28. F. M. Fowkes in K. L. Mittal and H. R. Anderson (Eds), *Acid-base Interactions:* Relevance to Adhesion Science and Technology, VSP, pp. 93 (1991)
- 29. U. Panzer and H.P. Schreiber Macromolecules 25 3633 1992
- 30. A. Voelkel, Macromolecular Symposia, (2003), 194, 27
- 31. G. W. Brindley and S. Yamanake American Mineralogy 64, 830 (1979).
- 32. M. Balogh and P. Laszlo *Organic Chemistry using Clays*. Springer-Verlag, Heidelberg (1993)
- 33. J. Schultz and L. Lavielle (1989) in D. R. Lloyd, T. C. Ward and H. P. Schreiber (Eds), Inverse Gas Chromatography: Characterisation of Polymers and Other Materials., Amer. Chem. Soc., pp. 185
- 34. C. Saint-Flour and E. Papirer Ind. Eng. Chem. Prod. Res. Dev. 21, 337, (1982).
- 35. C. Saint-Flour and E. Papirer Ind. Eng. Chem. Prod. Res. Dev. 21, 666, (1982).
- 36. D. M. Ansari and G. J. Price Polymer International in press.
- 35. D. M. Ansari and G. J. Price Submitted for publication (2003).

Table 1: Composition and structure of clay minerals used for IGC

		HYC	CAC / CAC-Sil
XRD analysis (%)	Kaolinite	98	Amorphous
Title unuiysis (70)	Quartz	2	-
BET Surface area (m <sup>2</sup> g <sup>-1</sup> )		8.8	7.0
Particle size (wt.%)	> 10 µm	0	5
	> 5 μm	2	15
	< 2 μm	82	49
Composition (wt.%)	SiO <sub>2</sub>	46.2	55.8
	Al <sub>2</sub> O <sub>3</sub>	39.2	41.0
	Fe <sub>2</sub> O <sub>3</sub>	0.23	0.59
	TiO <sub>2</sub>	0.09	0.06
	CaO	0.06	0.01
	MgO	0.07	0.19
	K <sub>2</sub> O	0.21	2.21
	Na <sub>2</sub> O	0.09	0.01
	Loss on ignition	13.8	0.30

**Table 2:** Comparison of the adsorption enthalpies for alkanes on kaolinites.

	Enthalpy of Adsorption (kJ mol <sup>-1</sup> )				
Probe	НҮС	CAC	CAC-Sil	Kaolinite*	Illite*
Pentane	$48 \pm 3$	$35 \pm 2$	$44 \pm 2$	50	42
Hexane	59 ± 4	$46 \pm 4$	$45 \pm 1$	62	51
Heptane	$69 \pm 4$	$58 \pm 3$	$52 \pm 1$	69	65
Octane	81 ± 5	$73 \pm 4$	$59 \pm 1$	79	

<sup>\*</sup>Results from Ref. 22

**Table 3:** Entropies of adsorption for alkanes on kaolinites.

	Entropy of Adsorption (J K <sup>-1</sup> mol <sup>-1</sup> )			
Probe	НҮС	CAC	CAC-Sil	
Pentane	- 90 ± 7	-70 ± 5	-90 ± 6	
Hexane	$-110 \pm 8$	$-87 \pm 5$	-83 ± 6	
Heptane	$-122 \pm 8$	$-106 \pm 6$	$-95 \pm 6$	
Octane	$-142 \pm 9$	$-133 \pm 8$	$-105 \pm 7$	

**Table 4:** Comparison of the dispersive surface free energy for kaolinites.

	Dispersive Component of Surface Free Energy (mJ m <sup>-2</sup> )				
Temp. (°C)	HYC	CAC	CAC-Sil	Kaolinite*	
80	165 ± 5	139 ± 4	$64 \pm 2$	154 – 211	
90	$156 \pm 6$	$137 \pm 3$	$58 \pm 2$		
100	$149 \pm 5$	$132 \pm 3$	$63 \pm 3$	167 – 201	
110			$65 \pm 3$		
120	151 ± 4	$130 \pm 2$	58 ± 2	156 – 212	
130			$56 \pm 2$		
140	$147 \pm 5$	$130 \pm 3$	$56 \pm 3$	160 - 217	

<sup>\*</sup> Results from Ref. 22

**Table 5:** Specific interaction energies\* for polar probes on clays.

	Variation in free energy of adsorption from the alkane line $(\Delta G_{sp}) \; (kJ \; mol^{\text{-}1})$			
Probe	$\frac{\text{HYC}}{(a(\gamma_1^{\ d})^{1/2} \text{ plot})}$	HYC (log P <sub>o</sub> plot)	CAC (log P <sub>o</sub> plot)	CAC-Sil (log Po plot)
Chloroform	$5.1 \pm 0.4$	$5.0 \pm 0.4$	-2.7	4.1
Tetrachloromethane	$-4.8 \pm 0.4$	$-4.9 \pm 0.4$	$-2.1 \pm 0.3$	2.2
THF	$21.5 \pm 1.0$	$18.2 \pm 0.9$	NPD	
Acetone	$8.5 \pm 0.3$	$4.3 \pm 0.3$	NPD	NPD
Ethyl acetate	$7.1 \pm 0.4$	$5.1 \pm 0.4$	NPD	NPD
Diethyl ether	$13.7 \pm 0.8$	$12.2 \pm 0.9$	NPD	
Cyclohexane		$-7.9 \pm 0.5$	$-4.3 \pm 0.6$	-2.5
Pentene			$4.9 \pm 0.6$	1.8
Hexene		$8.6 \pm 0.4$	$4.0 \pm 0.4$	1.8
Octene		$8.8 \pm 0.4$	$3.8 \pm 0.4$	1.8

<sup>\*</sup> NPD = no peak detected,

# **CAPTIONS FOR FIGURES**

**Figure 1**: Plot of  $\Delta G^{\circ}_{a}$  versus temperature for HYC to determine  $\Delta H^{\circ}_{a}$ 

**Figure 2:** Plot of  $\Delta G^{\circ}_{a}$  versus temperature for CAC to determine  $\Delta H^{\circ}_{a}$ 

**Figure 3:** Plot of  $\Delta$  G<sub>a</sub> versus temperature for CAC-Sil to determine  $\Delta$ H $^{\circ}$ <sub>a</sub>

**Figure 4:** Plot of  $RT ln V_n$  versus number of carbon atoms (from alkane probes) for HYC to determine  $\gamma_s^d$ 

**Figure 5:** Plot of  $\Delta$  G<sub>a</sub> versus a  $(\gamma_1^d)^{1/2}$  for HYC to determine specific interaction energies.

**Figure 6**: Plot of  $\Delta$  G<sub>a</sub> versus log P° for HYC to determine specific interaction energies.

Figure 7: Plot of  $\Delta G_a$  versus log  $P^o$  for CAC-Sil

# Supplementary data

**Figure S1**: Plot of RT*ln*V<sub>n</sub> versus number of carbon atoms (from alkane probes) for CAC.

**Figure S2:** Plot of RT*ln*V<sub>n</sub> versus number of carbon atoms (from alkane probes) for CAC-Sil.

**Figure S3:** Plot of  $\Delta G_a$  versus log  $P_o$  for CAC to determine specific interaction energies.

**Figure 1**: Plot of  $\Delta G^{\circ}_{a}$  versus temperature for HYC to determine  $\Delta H^{\circ}_{a}$ 

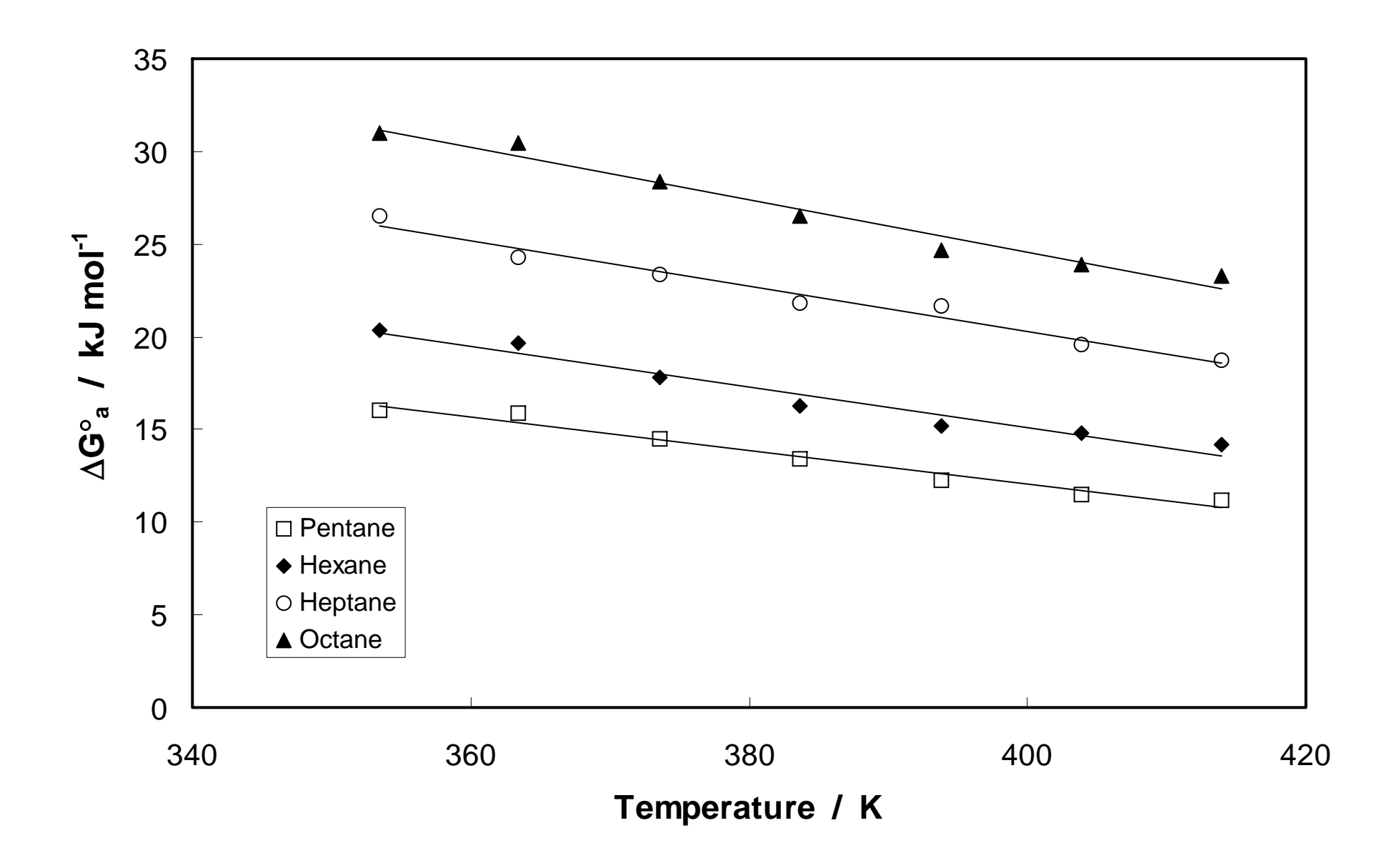


**Figure 2:** Plot of  $\Delta G^{\circ}_{a}$  versus temperature for CAC to determine  $\Delta H^{\circ}_{a}$ 

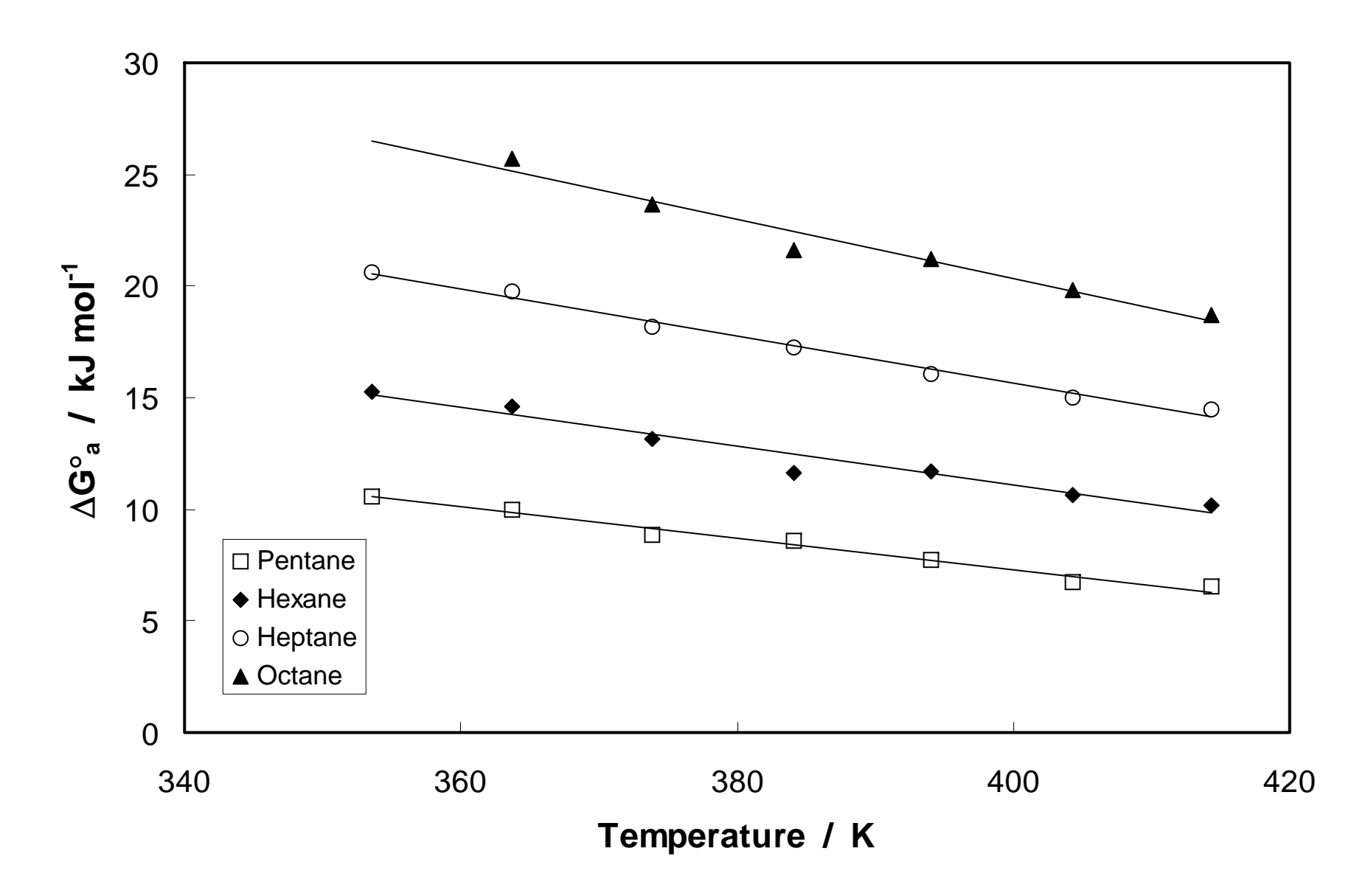


**Figure 3:** Plot of  $\Delta$  G<sub>a</sub> versus temperature for CAC-Sil to determine  $\Delta$ H°<sub>a</sub>

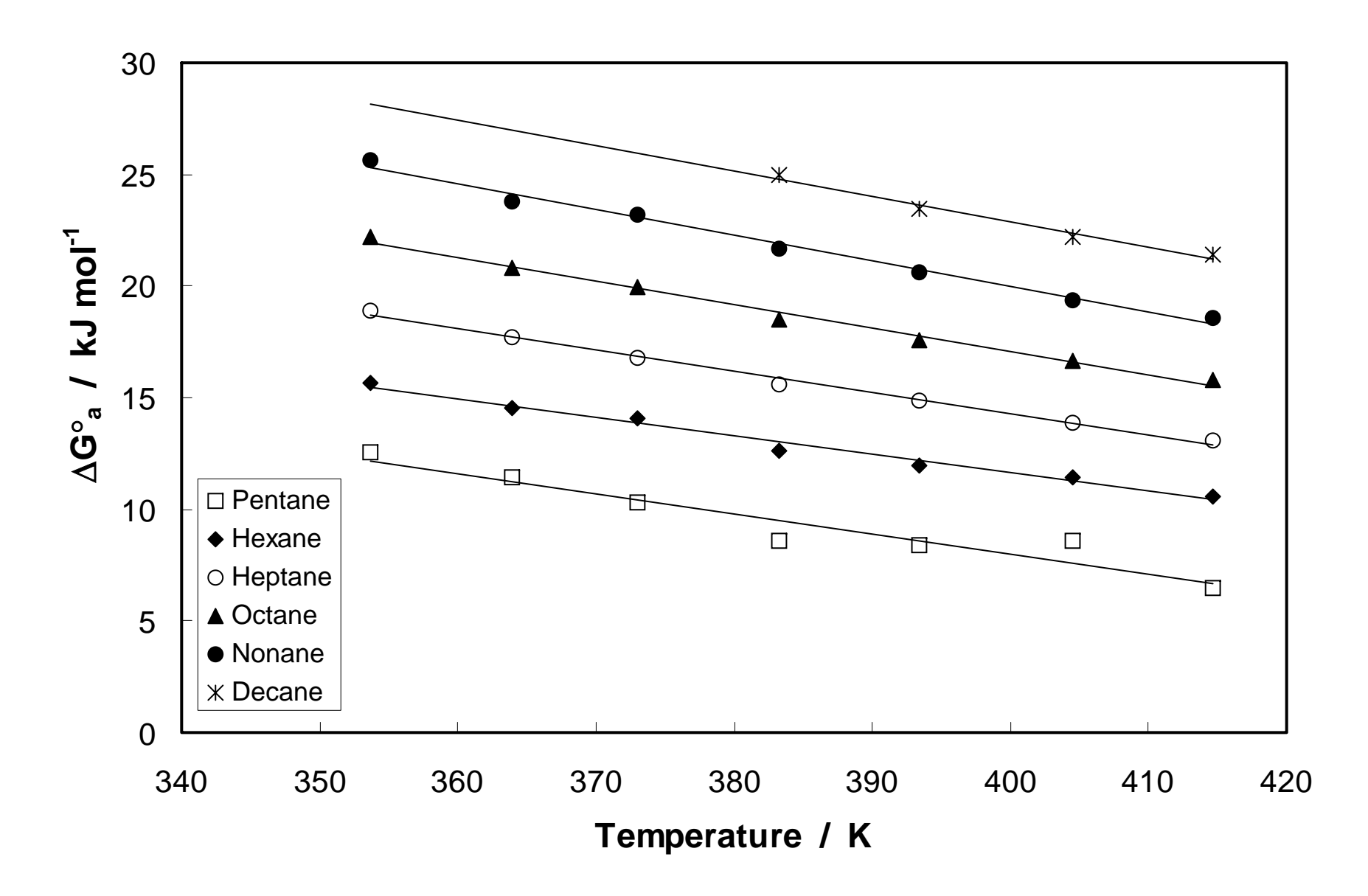


**Figure 4:** Plot of RTlnV<sub>n</sub> versus number of carbon atoms (from alkane probes) for HYC to determine  $\gamma_s^d$ 

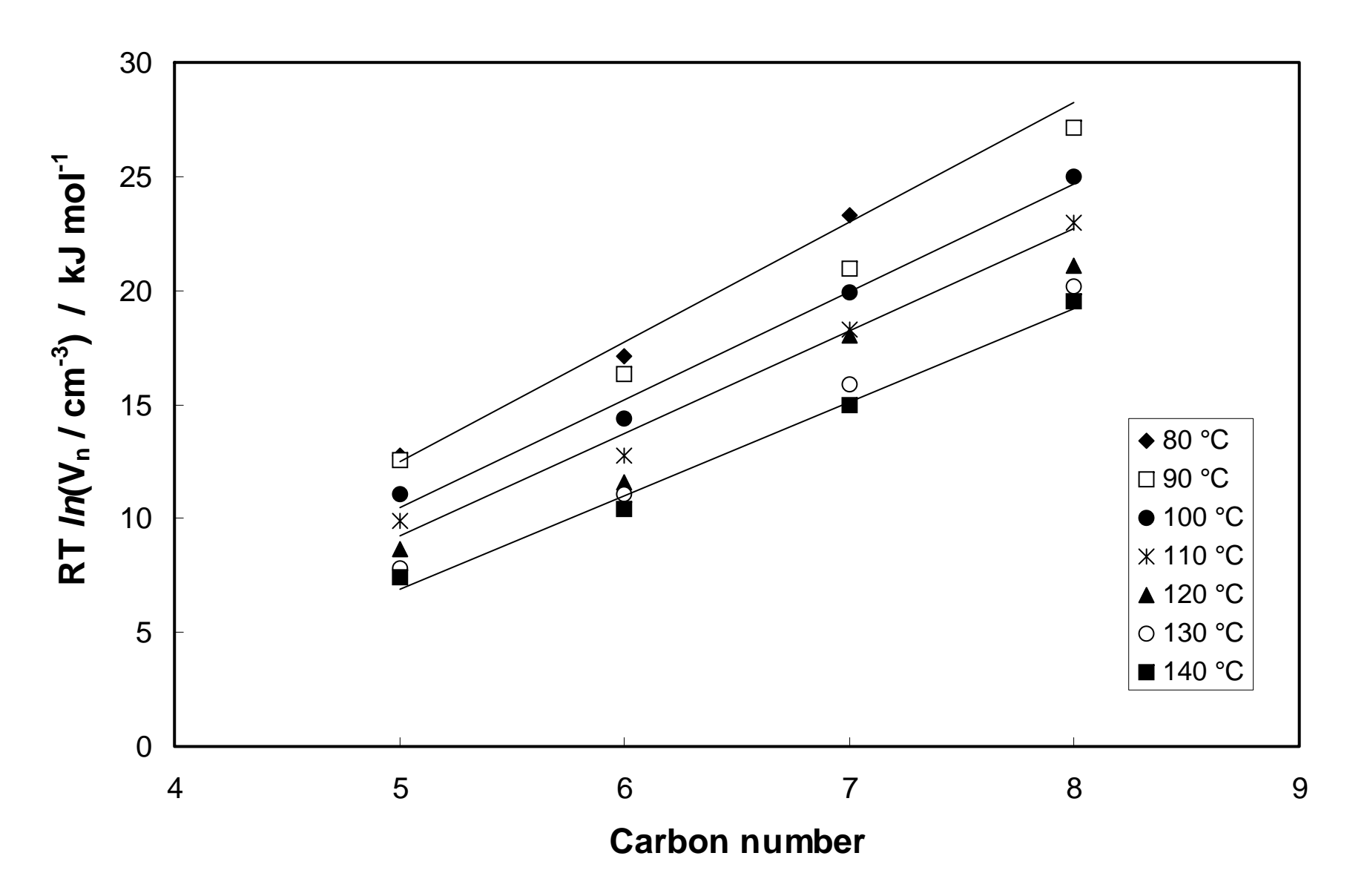


**Figure 5:** Plot of  $\Delta$   $G_a$  versus a  $(\gamma_1^d)^{1/2}$  for HYC to determine specific interaction energies.

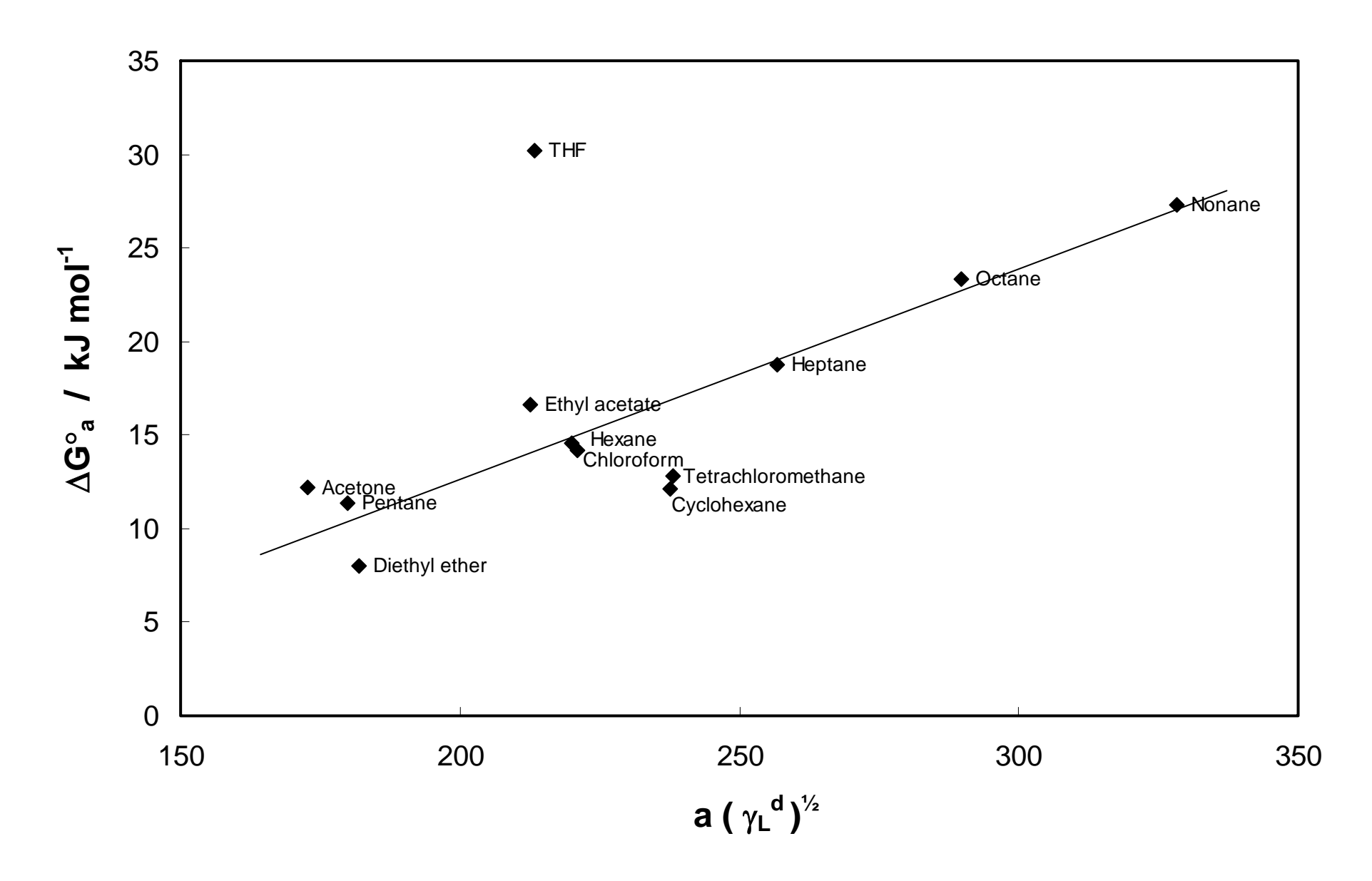


**Figure 6**: Plot of  $\Delta$  G<sub>a</sub> versus log P<sup>o</sup> for HYC to determine specific interaction energies.

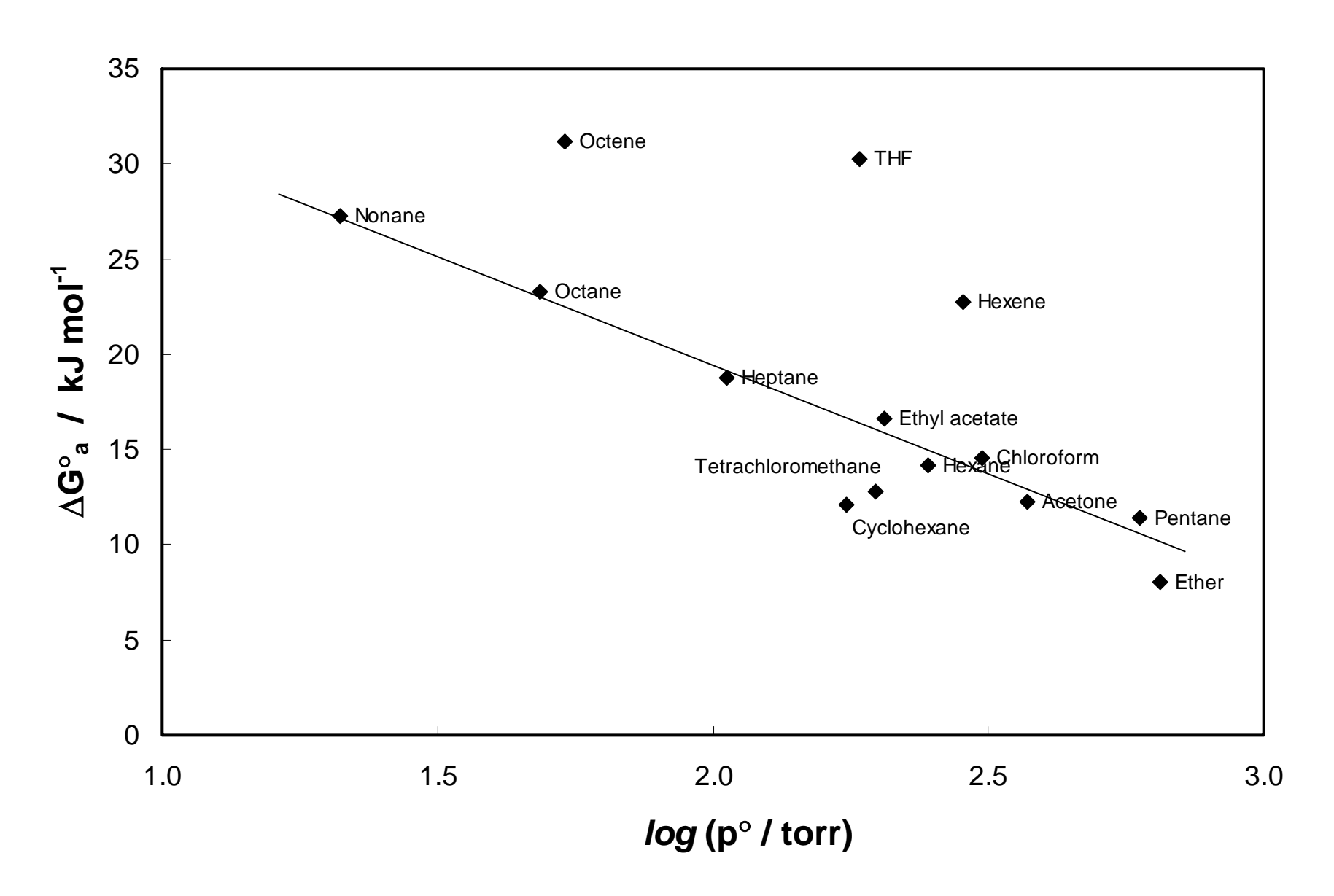


**Figure 7**: Plot of  $\Delta G_a$  versus log P° for CAC-Sil

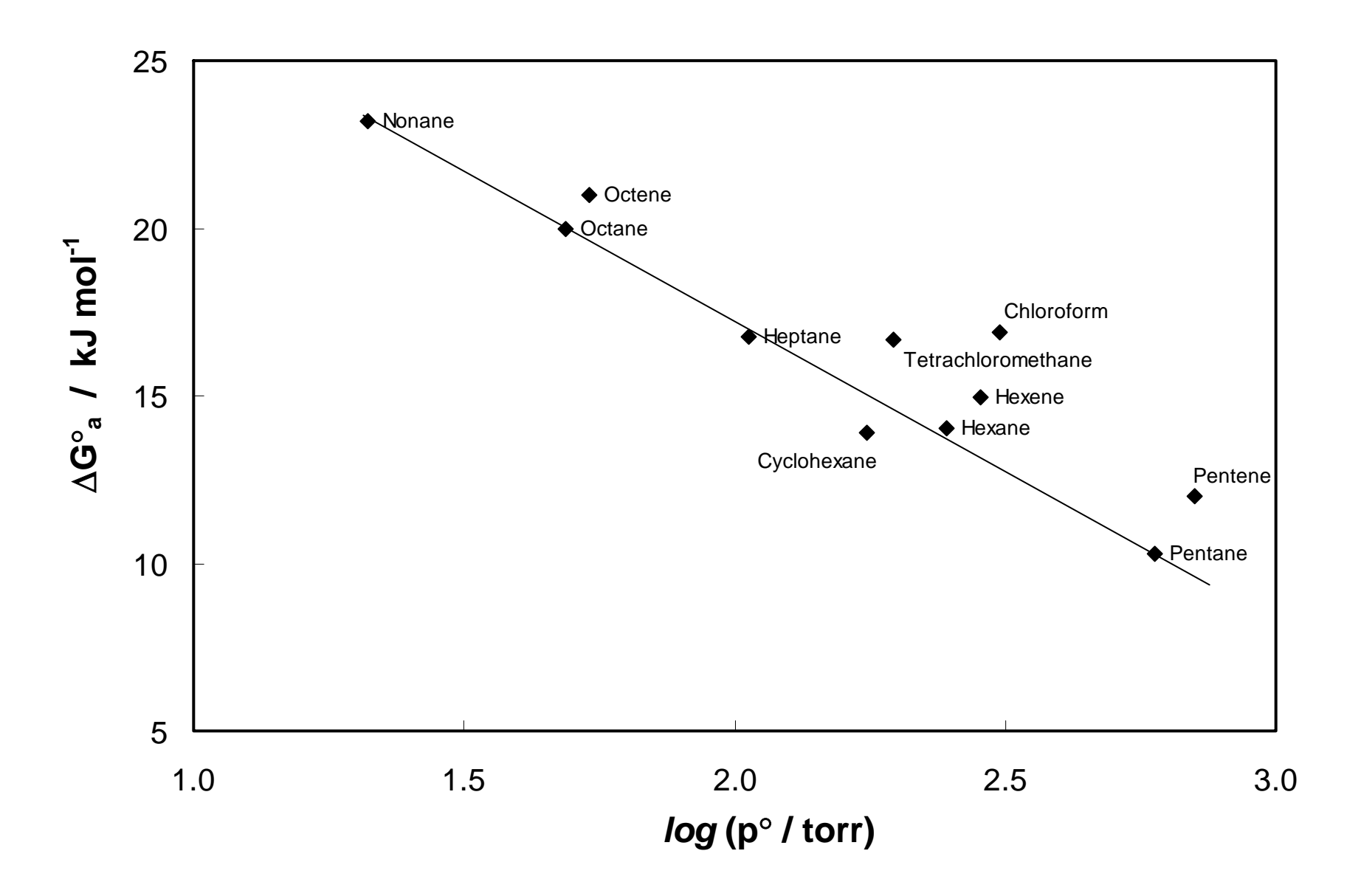


**Figure S1**: Plot of RT*ln*V<sub>n</sub> versus number of carbon atoms (from alkane probes) for CAC.

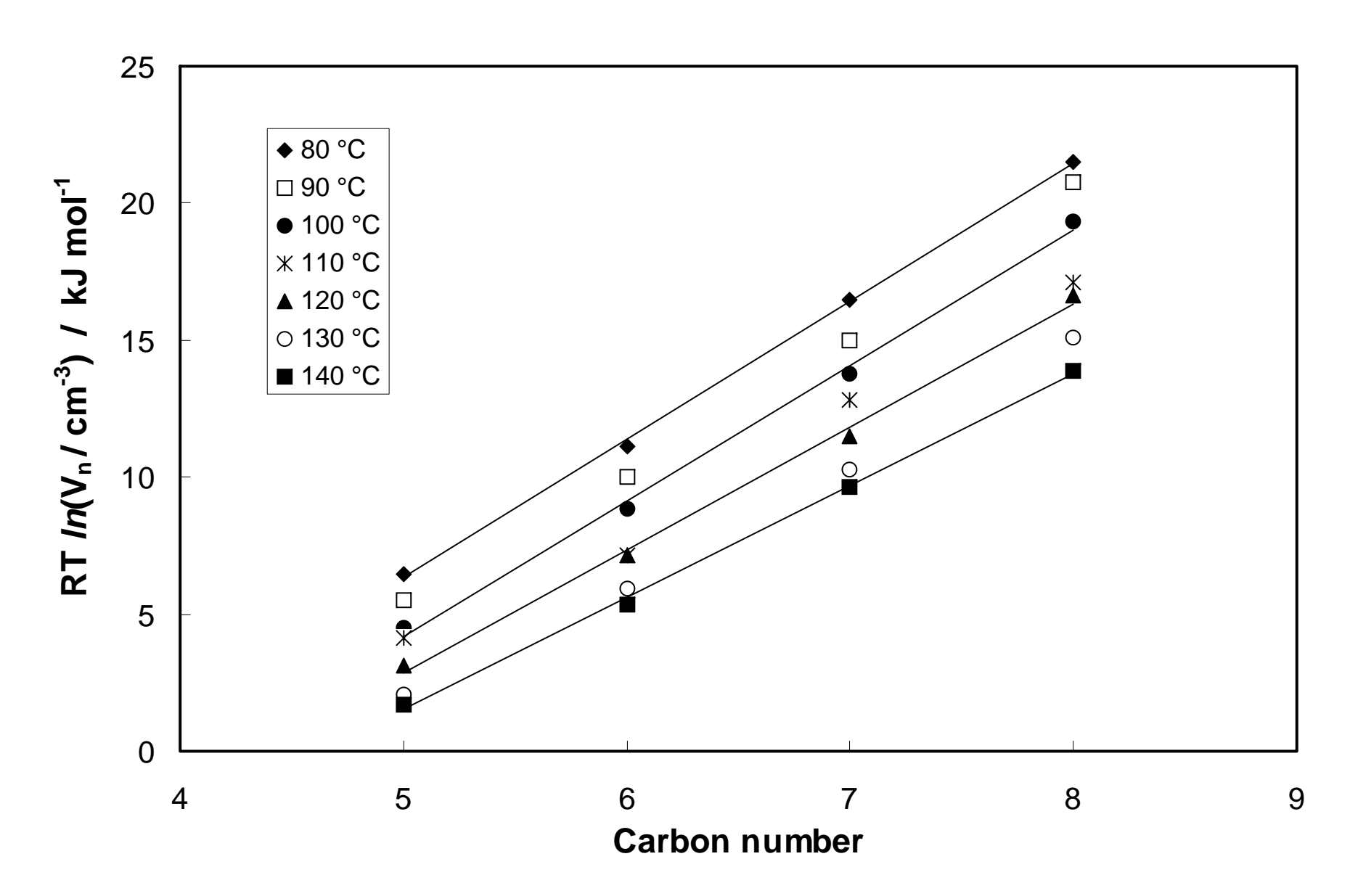
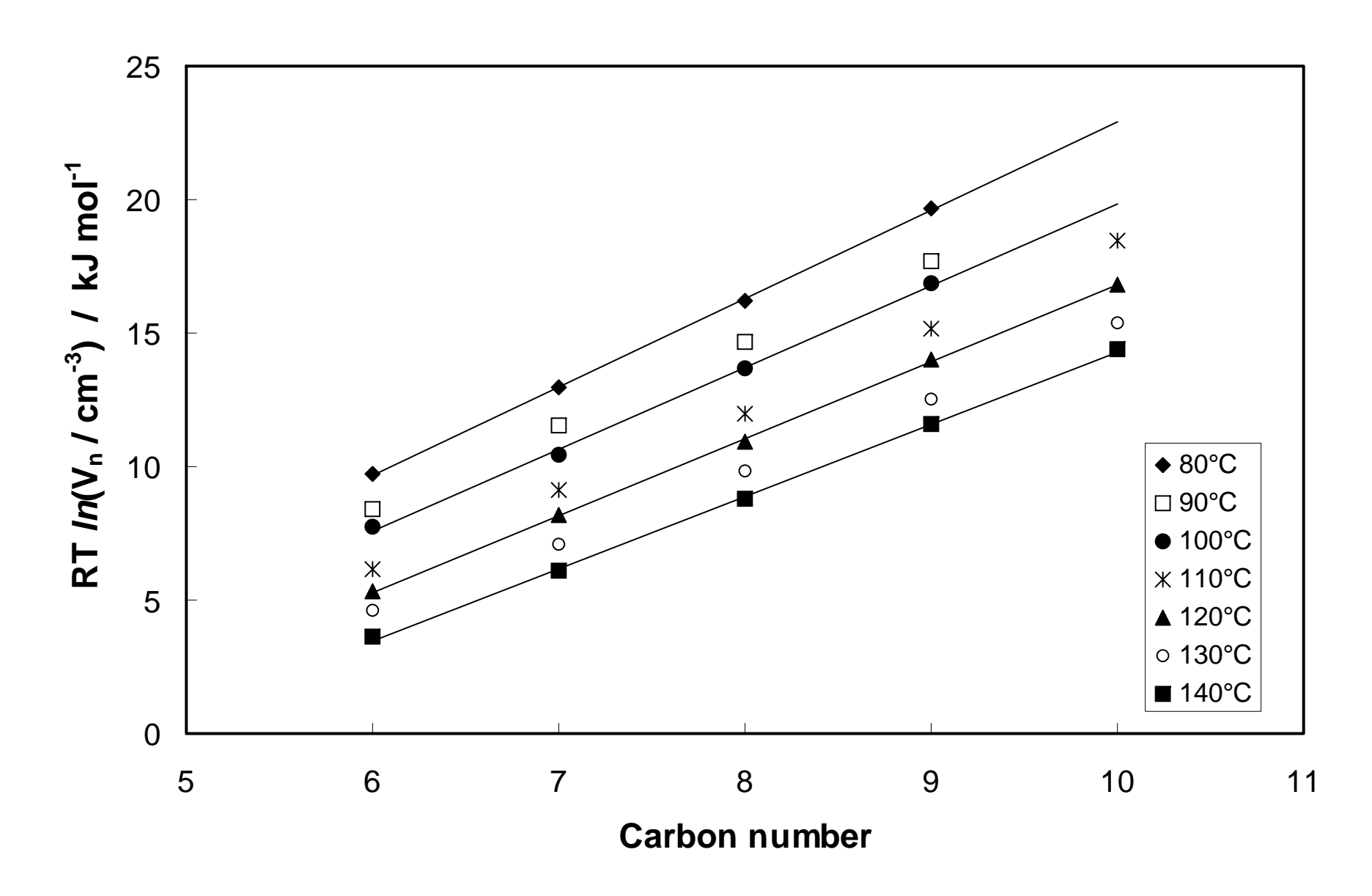


Figure S2: Plot of  $RTlnV_n$  versus number of carbon atoms (from alkane probes) for CAC-Sil.



**Figure S3:** Plot of  $\Delta G_a$  versus log  $P_o$  for CAC to determine specific interaction energies.

